

# Finite Element Modeling of Roller Burnishing Process

Y.C. Yen, P. Sartkulvanich, T. Altan (1)

Engineering Research Center for Net Shape Manufacturing (ERC/NSM),  
The Ohio State University, Columbus, Ohio, USA

## Abstract

Hard roller burnishing is a cost effective surface enhancement process where a ceramic ball rolls on the machined surface under a high pressure and flattens the roughness peaks. It not only improves surface finish but also imposes favorable compressive residual stresses and raises hardness in functional surfaces, which can lead to long fatigue life. Most research in the past focused on experimental studies. There is still a special need for a reliable finite element (FEM) model that provides a fundamental understanding of the process mechanics. In this study, 2D and 3D FEM models for hard roller burnishing were established. The simulation results (i.e. surface deformation and residual stress) were evaluated and compared between initial hard turned and burnished surfaces. The predicted residual stress was validated with the experimental data obtained from the literature.

## Keywords:

Roller, Finite Element Method (FEM), Burnishing

## 1 INTRODUCTION

The surface integrity of an engineered surface is generally characterized in terms of surface finish, state of residual stress, microstructure and microhardness. Generally, good surface finish, high compressive residual stress, and high hardness of the surface layer prolong the fatigue life of the components. During 1980's, the development of hard turning technology made it possible to replace at least some rough grinding with single-point cutting processes. However, the applications of hard turning as a finishing process are limited by tool wear. To broaden the capability of hard turning as a finishing process, it is practical to provide necessary surface modifications (i.e. improving surface finish and converting tensile residual stresses to compressive). Therefore, a hard roller burnishing would be best suitable since the burnishing tool can be readily installed on the same CNC machine setting.

Figure 1 illustrates a typical roller burnishing operation with a hydrostatically supported ball. The process is characterized by a single pass of a smooth free-rolling spherical ball (3-12 mm in diameter) under a normal force sufficient to deform the peaks of the surface profile. The ball is in contact only with the surface to be burnished and free to roll with very small friction. As in the cutting action, plastic deformation is produced over the entire surface as the tool continuously fed along the workpiece axis.

To implement a successful hard roller burnishing process, the effects of burnishing parameters on the surface finish and surface integrity need to be evaluated. Most research

in the past focused on experimental studies and analytical approaches. There is still a special need for a reliable FEM model that provides a fundamental understanding of the process and helps in optimizing burnishing conditions.

## 2 TECHNICAL BACKGROUND

### 2.1 Experimental Studies on Roller burnishing

In the past decades, research in roller burnishing was based on experimental studies. The research groups contributing to this field mainly include the WZL/RWTH, Aachen, Germany [1, 2], Ecoroll, Germany [3], the University of Toledo [4] and Lambda Research [5]. Experimental data have also been reported worldwide by many researchers [6 to 9].

For hard roller burnishing (hard turning plus roller burnishing), experiments indicate that nearly constant surface roughness can be achieved over a wide range of process conditions [2]. Burnishing can generate compressive residual stress throughout the surface layers although tensile residual stresses exist on the prior machined surfaces [2]. The process parameters of roller burnishing generally include 1) burnishing speed, 2) burnishing feed rate, 3) applied fluid pressure or normal force and 4) ball diameter. One of recent studies was reported in [1]. 100Cr6V samples (equivalent to AISI 52100) were first hardened, hard turned using tools with different amount of flank wear and then burnished using different burnishing conditions.

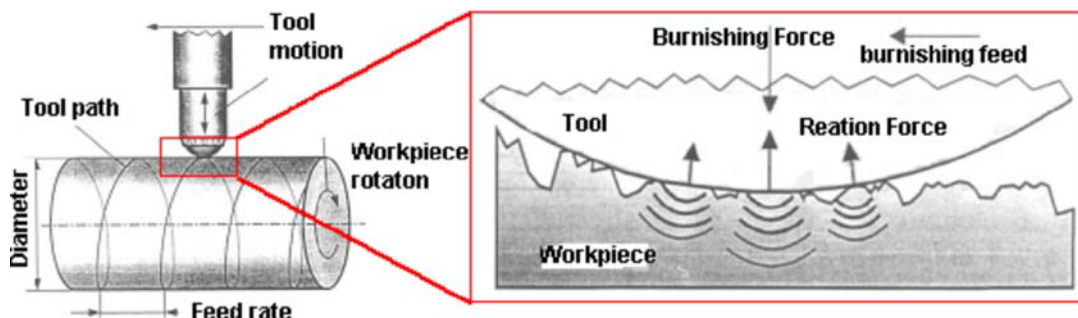


Figure 1: Roller burnishing process [1]

The following conclusions were drawn from [1]:

- Surface finish could be improved up to 70% with increasing burnishing pressure and decreasing workpiece hardness.
- The improvement of surface finish was not sensitive to (a) burnishing speed and (b) feed rate in the low range.
- High burnishing pressure and large ball diameter caused the surface residual stress to be more compressive with an increased penetration depth.
- Different initial residual stress distributions generated by hard turning did not significantly influence the residual stress behavior after roller burnishing.
- Burnishing pressures higher than 20 MPa result in an increase of surface hardness.

## 2.2 Finite Element Modeling of Roller Burnishing Process

In the same study [1], Roettger developed a 2D FEM model for roller burnishing using commercial FEM software "DEFORM-2D®". In this model, a rigid ball was pressed down on the rough workpiece surface until the reaction force reached a predefined value that is equal to the applied burnishing force. Then, the ball was lifted up from the surface and moved horizontally by the distance of the burnishing feed, Figure 2. However, this force-control model would underestimate the ball penetration depth because of line contact (due to the plane strain condition).

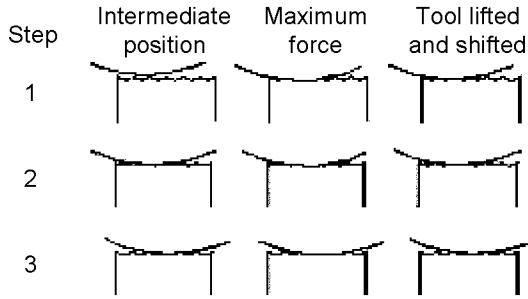


Figure 2: Simulation sequence for 2-D FEM modeling of roller burnishing [1]

## 3 DEVELOPMENT OF 2D FEM MODELING

In the present study, the model from [1] has been further improved. FEM commercial software "DEFORM 2D®" is used. The procedure for modeling roller burnishing as a simplified 2D process is illustrated in Figures 3. Figure 3a shows a 3D roller burnishing process. The geometry of the original surface prior to burnishing is given in Figure 5. Plane (W) is assumed to pass through the center of the ball along one roughness ridge. Figure 3b shows the motion viewed on the section plane (W). The symbol  $D$  is the ball penetration depth.

To simulate the deformation process for the material element moving from  $A_0$  to  $A_2$ , the 3D rolling motion of the ball may be virtually transformed into a translational motion in Z direction in the proposed 2D model representing the

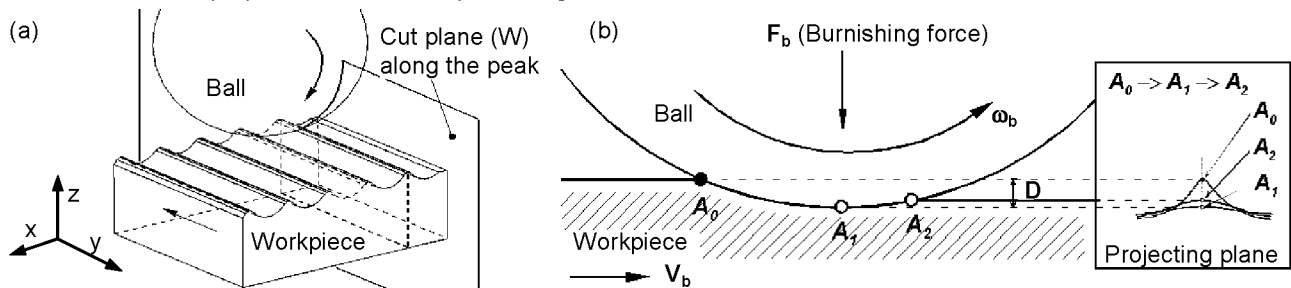


Figure 3: (a) Roller burnishing process; (b) schematics of burnishing motion on the plane W

projecting plane (small window in Figure 3b). The surface roughness profile, generated by turning, and the effect of burnishing feed rate can be easily implemented in this 2D model.

The movement of the ball in the simulation can be controlled by using two types of control curves: (1) the time variation of the normal reaction force on the tool (force control) or (2) the time variation of the vertical displacement of the tool (displacement control). The limitation of the force control method used in [1] is that the final penetration depth of the ball under the plane strain condition (i.e. line contact) will actually be smaller than it would have been under the realistic 3D condition with the same applied force. Thus, it is more reasonable to use the displacement control method. Since this method required the information on the maximum ball penetration depth, a series of 3D ball burnishing simulations were conducted to determine the relationship between burnishing force and ball penetration depth (Figure 4).

The following burnishing conditions were used:

- Burnishing ball diameter ( $d_b$ ) = 6 mm
- Burnishing pressure ( $p_b$ ) = 40 MPa (giving a burnishing force  $F_b = \pi r_b^2 p_b = 1131$  N)
- Burnishing speed ( $V_b$ ) = 100 m/min
- Burnishing feed rate ( $f_b$ ) = 0.06 mm/rev

To employ a realistic ball contact time, the time interval for each simulation cycle is approximated from the burnishing speed and the diameter of the projected contact circle corresponding to the maximum penetration depth, by " $t_c = d_c/V_b$  (in the order of milliseconds)". " $d_c$ " is the diameter of the projected contact circle. For a given burnishing force, the penetration depth ( $D$ ) of 0.027 mm was obtained from Figure 4. The projected diameter of contact cycle at the depth  $D$  and the contact time can be simply calculated. Assuming a parabolic relation, the obtained displacement as a function of time is  $D(t) = -464868.029(t-0.000241)^2 + 0.027$  mm. Details are given in [10].

The theoretical mean peak-to-valley height ( $R_{z,th}$ ) of the initial surface geometry can be calculated from the cutting feed rate ( $f$ ) and the size of tool nose radius ( $r_e$ ) used in turning operation as expressed by Eq. (1).

$$R_{z,th} = r_e \cdot \left[ 1 - \sqrt{1 - (f/(2r_e))^2} \right] \approx f^2/(8r_e) \quad (1)$$

As shown in Figure 5, the distance between two roughness peaks is 0.18 mm and the calculated mean peak-to-valley height ( $R_z$ ) is 0.011 mm. In order to minimize the boundary effect, the workpiece height is 2 mm and the width is 4 mm. Figure 5 also displays the displacement constraints that were applied on the left, right, and bottom boundaries of the workpiece. In [1], only 4 simulation cycles were used. However, the proposed model uses 10 simulation cycles in order to take into account the full deformation history of a single surface asperity during burnishing.

The material flow stress properties of the hard turned surface layer for AISI 52100 (62 HRC), initially used in [1], were used in this study, as shown in Eq. (2).

$$\bar{\sigma} = 300\bar{\varepsilon}_p^{0.3\dot{\varepsilon}_p^{0.1}} + 2500 \quad \text{MPa} \quad (2)$$

where  $\bar{\sigma}$  = flow stress (in MPa),  $\bar{\varepsilon}_p$  = plastic strain and  $\dot{\varepsilon}_p$  = plastic strain rate

Figure 6 shows a comparison of the three flow stress models proposed in [1; 11; and 12]. Similarity can be observed in terms of the yield strength and yield strain values; however, strain hardening is more significant for the data in [11] and [12].

Both 2D and 3D models consider the ball as a rigid object and the workpiece as an elasto-plastic object. A small Coulomb coefficient of friction of  $1 \times 10^{-5}$  was assumed for free rolling process. The temperature rise in the workpiece due to plastic deformation at the surface is neglected.

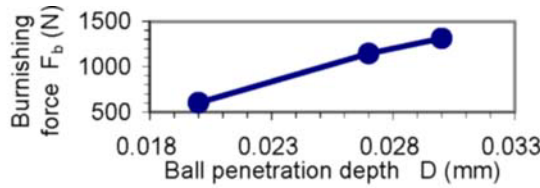


Figure 4: Relationship between the ball burnishing force and the penetration depth from 3D burnishing simulations

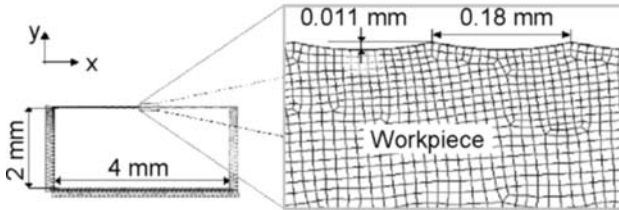


Figure 5: Dimensions of the workpiece for 2D simulations and the initial surface geometry

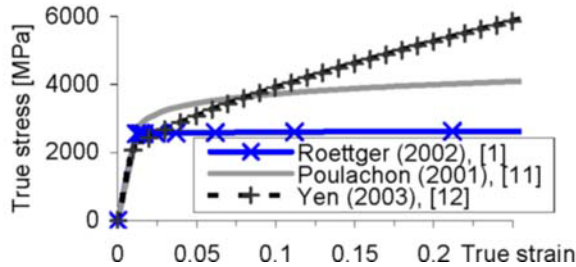


Figure 6: Comparison of room-temperature flow stress curves derived from material models provided in [1; 11; and 12], for hardened AISI 52100 steel (58-62 HRC)

#### 4 DEVELOPMENT OF 3D FEM MODELING

The FEM software “DEFORM-3D®” was used. The 3D model requires a very fine mesh resolution for the workpiece surface (at least 8-12 elements between two roughness peaks). Workpiece object is based on four-node linear tetrahedral solid elements. Figure 7 presents the 3D burnishing simulation model used in this study. Similar to 2D model, the surface roughness profile is calculated, Eq. (1). The surface curvature effect of a cylindrical workpiece and the effect of helical cutting path angle were neglected. In this model, the ball moves towards the workpiece at the assigned burnishing speed. Referring to Figure 3a, fixed displacement boundary conditions were assigned at the bottom ( $v_x=v_y=v_z=0$ ), the left ( $v_x=0$ ), the right ( $v_x=0$ ) and the back ( $v_y=0$ ) of the workpiece object.

The ball penetration depth needs to be adjusted during the simulation to generate a normal load that matches the applied burnishing force. The ball penetration depth for the first burnishing pass was 0.27 mm. For subsequent passes, the penetration depth is larger because the burnishing action only takes place on one side of the ball.

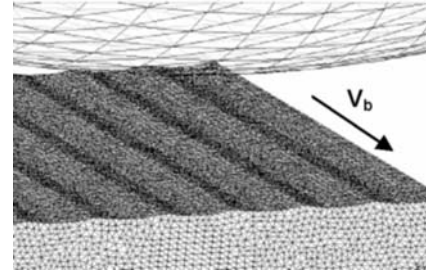


Figure 7: 3D roller burnishing FEM model

#### 5 SIMULATION RESULTS AND DISCUSSION

##### 5.1 Results of 2D FEM Model

Surface roughness and residual stress of the burnished surface are analyzed. Figure 8 shows the surface roughness profiles of 2D model at the start, middle and end stages of burnishing process. The results indicate that the surface roughness has been smoother by burnishing; with the roughness depth ( $R_z$ ) reduced from 11 to 1  $\mu\text{m}$ .

Four characteristic vertical sections passing through the peak, the valley, and two points (1/4 and 3/4 pitch unit away from the peak) were selected. The residual stresses over the depth from these four sections were averaged. As shown in Figure 9, for the tangential stress, the 2D model predicted the location of a maximum compressive residual stress in agreement with the experiment while the maximum compressive residual stress value is larger than that in the experiment. For the axial stress, simulations predicted the maximum compressive residual stress near the same depth as compared to the experiment. However, unlike the experimental curve, the stresses drastically turned into high positive stress levels when approaching the surface.

##### 5.2 Results of 3D FEM Model

Figure 10 presents a 2D view of the predicted surface geometry after seven burnishing passes from 3D burnishing model, compared to the original surface geometry. Similar to the 2D results, the surface is smoothed and the profile peak is slightly shifted to the feeding end of the ball. However, the peaks are displaced off opposite to the direction of burnishing speed because of pure rolling action. Results of 3D simulation show that the level of the burnished surface is considerably lower than that of the original surface due to three possible reasons. First, the plane strain assumption for the 2D model prohibits the materials from flowing along the out-of-plane (tangential) direction. Second, due to the loss of materials in the longitudinal plane (corresponding to the 2D simulation), the elastic relaxation of the surfaces in the 3D model was much less significant. Third, the varying penetration depth of the ball in the 3D simulation was larger than the constant penetration depth defined in the 2D simulation, except in the first burnishing pass.

For overall results of the residual stress prediction, the refined 2D model seems to give better results compared to the 3D model. The 3D model tends to predict the maximum compressive stress at shallower depths (Figure 11). The release of the fixed displacement boundary constraints on the workpiece only contributed to an upward shift of the predicted residual stress curves (Figure 11). These changes in the stress level due to the boundary effect

imply that the workpiece modeled in the 3D simulation was undersized in the thickness direction.

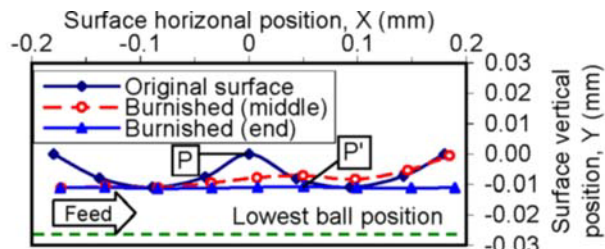


Figure 8: Predicted surface roughness profiles from 2D model (P & P': the peak before and after roller burnishing)

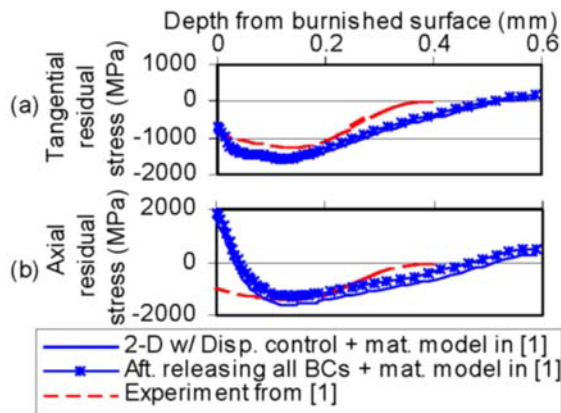


Figure 9: Comparison of residual stress from the 2D model and the experimental data given in [1]

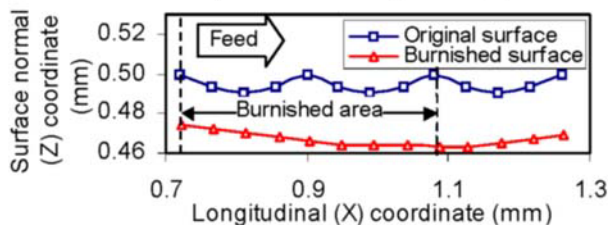


Figure 10: Comparison of the deformed surface geometry from the 3D model with the original surface geometry

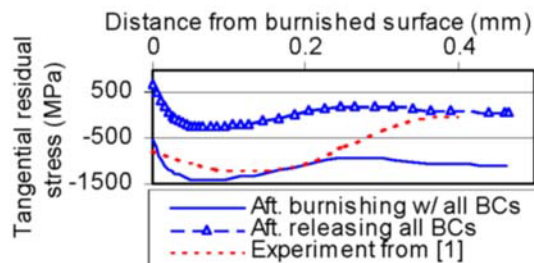


Figure 11: Comparison of tangential residual stress predicted by the 3-D model before and after releasing BCs

## 6 SUMMARY

Results of this study can be summarized as follows:

- 2D and 3D FEM models of roller burnishing are successfully established.
- The refined 2D model seems to predict the residual stresses better than the 3D model.
- The changes in the stress level due to the release of the fixed displacement boundary constraints on the workpiece were more significant for the 3D model, which implies that the workpiece model was too thin.
- The 3D model showed more realistic surface deformation and material flow, whereas the simplified 2D model represents a series of "indenting" cycles.

Future work will include the following:

- Development of an inverse engineering method and Instrumented Indentation Tests (IIT) to determine the properties of the turned surface layer
- Improvements of existing 2D and 3D FEM models (e.g. a new 3D simulation with thicker workpiece model and tool rolling motion, 2D simulations with initial stress/strain data from turning).
- Additional hard turn and burnishing experiments.
- Implementing a design of experiment (DOE) technique to optimize ball burnishing process parameters upon surface finish and residual stress

## 7 ACKNOWLEDGMENTS

This paper summarizes the research conducted under the ongoing NSF funded project (Grant No. 0323631). This support is gratefully acknowledged.

## 8 REFERENCES

- [1] Roettger, K., 2002, Walzen hartgedrehter Oberflächen, PhD Dissertation, WZL, RWTH Aachen
- [2] Klocke, F., Liermann, J., 1998, Roller Burnishing of Hard Turned Surfaces, *International Journal of Machine Tools and Manufacture*, 38/5-6: 419-423
- [3] ECOROLL AG Werkzeugtechnik, 1996, Application Description: Deep Rolling. ECOROLL AG Research Report Nr. AO-4088/1E: 1-15.
- [4] Luca, L., 2002, Investigation into the Use of Ball Burnishing of Hardened Steel Components as a Finishing Process, PhD Dissertation, U. of Toledo
- [5] Prevé, P.S., Ravindranath, R.A., Shepard, M., Gabb, T., 2003, Case Studies of Fatigue Life Improvement Using Low Plasticity Burnishing in Gas Turbine Engine Applications, *Proceedings of ASME Turbo Expo*, June 16-19, Atlanta, Georgia, USA
- [6] Hassan A.M., Maqableh, A.M., 2000, The Effects of Initial Burnishing Parameters on Non Ferrous Components, *Journal of Materials Processing*, 102: 115-121
- [7] El-Axir, M.H., El-Khabeery, M.M., 2003, Influence of Orthogonal Burnishing Parameters on Surface Characteristics for Various Materials, *Journal of Materials Processing Technology*, 132: 82-89
- [8] Némat, M., Lyons, A. C., 2000, An Investigation of the Surface Topography of Ball Burnished Mild Steel and Aluminum, *International Journal of Advanced Manufacturing Technology*, 16: 469-473
- [9] Shiou, F.J., Chen, C. H., 2003, Determination of Optimal Ball Burnishing Parameters for Plastic Injection Moulding Steel, *International Journal of Advanced Manufacturing Technology*, 3: 177-185
- [10] Yen, Y.C., Altan, T., 2004, Finite Element Modeling of Ball Burnishing – Prediction of Surface Deformation and Residual Stress, *ERC Report No. HPM/ERC/NSM-04-R-04*, Ohio State University
- [11] Poulachon, G., Moisan, A., Jawahir, I.S., 2001, On Modelling the Influence of Thermo-Mechanical Behavior in Chip Formation During Hard Turning of 100Cr6 Bearing Steel, *Annals of the CIRP*, 50/1: 31-36
- [12] Yen, D., Private Communication on "Enabling Technologies for lean manufacturing of critical hardened steel applications", June 2003